J|A|C|S
ARTICLES
Published on Web 09/19/2007

H-ras Protein in a Bilayer: Interaction and Structure Perturbation

Alemayehu A. Gorfe,*,† Arneh Babakhani,† and J. Andrew McCammon†,‡,§

Contribution from the Department of Chemistry and Biochemistry, Howard Hughes Medical Institute, and Department of Pharmacology, University of California at San Diego, La Jolla, California 92093-0365

Received May 31, 2007; E-mail: abebe@mccammon.ucsd.edu

Abstract: Ras GTPases become functionally active when anchored to membranes by inserting their lipid modified side chains. Their role in cell division, development, and cancer has made them targets of extensive research efforts, yet the mechanism of membrane insertion and the structure of the resulting complex remain elusive. Recently, the structure of the full-length H-ras protein in a DMPC bilayer has been computationally characterized. Here, the atomic interactions between the H-ras membrane anchor and the DMPC bilayer are investigated in detail. We find that the palmitoylated cysteines and Met182 have dual contributions to membrane affinity: hydrogen bonding by their amides and van der Waals interaction by their hydrophobic side chains. The polar side chains help maintain the orientation of the anchor. Although the overall structure of the bilayer is similar to that of a pure DMPC, there are localized perturbations. These perturbations depend on the insertion depth and backbone localization of the anchor, which in turn is modulated by the catalytic domain and the linker. The pattern of anchor amide-DMPC phosphate/carbonyl hydrogen bonds and the flexibility of Palm184 are important in discriminating between different modes of ras-DMPC interactions. The results provide structural arguments in support of the proposed participation of ras in the organization of membrane nanoclusters.

Introduction

Ras proteins mediate signaling pathways that control cell proliferation, development, and apoptosis; their malfunction is associated with a variety of cancers.[1] Therefore, much effort has been made toward understanding the thermodynamics and kinetics of membrane targeting by ras proteins and peptides derived from them.[2−5] These efforts would be greatly facilitated by knowledge of the structure of ras in a membrane and of the mechanism of ras−membrane complex formation. Such data are particularly crucial for the design of selective inhibitors against a variety of diseases, including anticancer agents that specifically target N-, K-, or H-ras.[6−9]

The small (189 amino acids) GTP hydrolyzing ras proteins are posttranslationally lipid modified to achieve stable binding to membranes, especially the plasma membrane. In the case of H-ras, it is first farnesylated at Cys186 via a thioether linkage, which is followed by proteolysis of the last three amino acids and carboxymethylation of the C-terminus. A subsequent double palmitoyl modification of adjacent cysteines forms a mature anchor for plasma membrane targeting (Figure 1A). Partly because palmitoylation is a reversible thioester linkage that can be selectively cleaved by enzymes such as palmitoylthioesterases,[10] there is a continuous recycling of H-ras between the plasma membrane and inner membranes.[11]

The structure and dynamics of membrane-bound full-length H-ras (residues 1−186) have been recently characterized using modeling and molecular dynamics (MD) simulations.[12] The study provided the overall picture of H-ras binding to a DMPC bilayer and identified residues in the linker and the catalytic domain that play a role in membrane binding. On the other hand, it has been shown that the minimal C-terminal heptapeptide (residues 180−186, ANCH, see Figure 1A) also binds stably to plasma membranes.[13,14] Its membrane affinity and lateral segregation properties, however, were found to be modulated by the catalytic domain (G-domain, residues 1−166) and the linker (residues 167−179).[13,15,16] However, lack of a membrane-

† Department of Chemistry and Biochemistry.
‡ Howard Hughes Medical Institute.
§ Department of Pharmacology.

(1) ten Klooster, J. P.; Hordijk, P. L. *Biol. Cell* **2007**, *99*, 1−12.
(2) Silvius, J. R. *J. Membr. Biol.* **2002**, *190*, 83−92.
(3) Shahinian, S.; Silvius, J. R. *Biochemistry* **1995**, *34*, 3813−22.
(4) Silvius, J. R.; l'Heureux, F. *Biochemistry* **1994**, *33*, 3014−22.
(5) Silvius, J. R.; Leventis, R. *Biochemistry* **1993**, *32*, 13318−26.
(6) Brunsveld, L.; Kuhlmann, J.; Waldmann, H. *Methods* **2006**, *40*, 151−65.
(7) Peters, C.; Wagner, M.; Volkert, M.; Waldmann, H. *Naturwissenschaften* **2002**, *89*, 381−90.
(8) Kadereit, D.; Kuhlmann, J.; Waldmann, H. *ChemBioChem* **2000**, *1*, 144−69.
(9) Volkert, M.; Wagner, M.; Peters, C.; Waldmann, H. *Biol. Chem.* **2001**, *382*, 1133−45.
(10) Linder, M. E.; Deschenes, R. J. *Biochemistry* **2003**, *42*, 4311−20.
(11) Rocks, O.; Peyker, A.; Kahms, M.; Verveer, P. J.; Koerner, C.; Lumbierres, M.; Kuhlmann, J.; Waldmann, H.; Wittinghofer, A.; Bastiaens, P. I. *Science* **2005**, *307*, 1746−52.
(12) Gorfe, A. A.; Hanzal-Bayer, M.; Abankwa, D.; Hancock, J. F.; McCammon, J. A. *J. Med. Chem.* **2007**, *50*, 674−684.
(13) Rotblat, B.; Prior, I. A.; Muncke, C.; Parton, R. G.; Kloog, Y.; Henis, Y. I.; Hancock, J. F. *Mol. Cell. Biol.* **2004**, *24*, 6799−810.
(14) Jaumot, M.; Yan, J.; Clyde-Smith, J.; Sluimer, J.; Hancock, J. F. *J. Biol. Chem.* **2002**, *277*, 272−8.
(15) Roy, S.; Plowman, S.; Rotblat, B.; Prior, I. A.; Muncke, C.; Grainger, S.; Parton, R. G.; Henis, Y. I.; Kloog, Y.; Hancock, J. F. *Mol. Cell. Biol.* **2005**, *25*, 6722−33.

10.1021/ja073949v CCC: $37.00

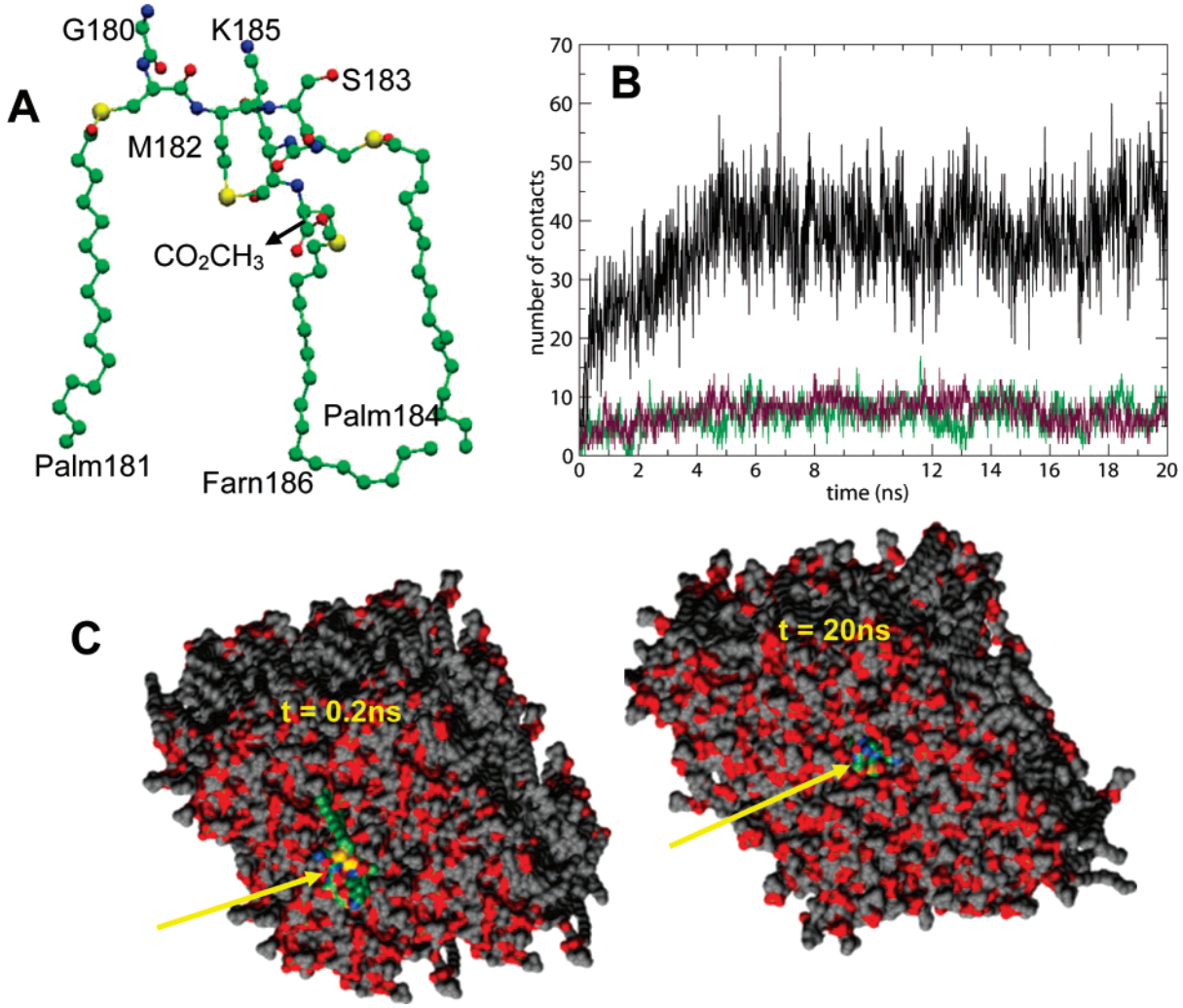

Figure 1. (A) Structure of H-ras membrane anchor (ANCH) from a simulation. Side chains of the polar (S183 and the N-terminal G180) and charged (K185) residues point up toward solvent. The palmitoylated (Palm181 and Palm184), hexadecylated (Farn186, which models a farnesyl group), and the nonpolar (Met182) residues are directed toward the hydrocarbon core. (B) Progress of ANCH membrane insertion during a 20 ns simulation. Insertion is measured by the number of contacts between all ANCH non-hydrogen atoms and acyl carbon (black), phosphate oxygen (dark green), and carbonyl (maroon) DMPC atoms. Contact is defined as the number of DMPC non-hydrogen atoms within 4 Å of any protein non-hydrogen atom. (C) Snapshots at 0.2 and 20 ns. The peptide is indicated by arrow. In this and subsequent figures, water and hydrogen atoms are omitted for clarity, ANCH is colored as shown in (A) and contact is defined as shown in (B), unless specified otherwise.

bound 3D structure of ras prohibited a deeper investigation of the atomic interactions that underlie these observations. It is therefore important to compare the structure and dynamics of the membrane-bound anchor with and without the linker and/or the catalytic domain. Furthermore, it has been proposed that membrane-bound ras is involved in the formation of signaling competent nanoclusters.[17−19] Therefore, a detailed investigation of the atomic interactions responsible for ras-induced membrane structure perturbation is needed.

In this paper we present results from MD simulations on the insertion of the anchor into a DMPC bilayer together with analysis of several previous simulations on the full-length H-ras and its hypervariable region.[12] We investigate the relationships among membrane-insertion depth, backbone localization, and membrane perturbation and provide structural arguments in support of the proposed participation of ras in the organization of membrane nanoclusters.[17−19]

Methods

An earlier work dealt with the full-length H-ras protein in its GDP- (H-ras-GDP) and GTP-bound (H-ras-GTP) forms as well as the hypervariable region (HVR).[12] HVR comprises the flexible linker (residues 167−179) and the anchor (residues 180−186). The binding of each system to a bilayer of 215 DMPC lipids was investigated using MD simulations; the simulations were named *fl.gdp*, *fl.gtp*, and *hvr*, respectively. Comparisons were made with control simulations of pure DMPC and the catalytic domain (residues 1−166) in water.[12] For each system (of up to ∼75 000 atoms), multiple simulations of 10−40 ns were carried out. Here, an insertion simulation of only the minimal membrane binding segment, or anchor (ANCH, Figure 1A), was run for 20 ns and is referred to as simulation *anch*. Details of the simulation procedure have been described before.[12] Briefly, after cycles of minimizations and equilibrations, the production simulations were performed at constant temperature (310 K), normal pressure, and cross-sectional area conditions. Periodic boundary conditions with full

(16) Plowman, S. J.; Hancock, J. F. *Biochim. Biophys. Acta* **2005**, *1746*, 274−83.
(17) Nicolau, D. V.; Jr.; Burrage, K.; Parton, R. G.; Hancock, J. F. *Mol. Cell. Biol.* **2006**, *26*, 313−23.
(18) Plowman, S. J.; Muncke, C.; Parton, R. G.; Hancock, J. F. *Proc. Natl. Acad. Sci. U.S.A.* **2005**, *102*, 15500−5.
(19) Hancock, J. F. *Nat. Rev. Mol. Cell Biol.* **2006**, *7*, 456−62.

particle-mesh Ewald electrostatics, a 12 Å cutoff for the van der Waals (vdW) interactions, a 14 Å cutoff for a nonbonded list update, the SHAKE algorithm, a 2 fs time step, the CHARMM27[20] force field, and the program NAMD[21] were used.

Results and Discussion

The two modes of ras binding to a DMPC bilayer that were previously proposed[12] differ in the orientation of the catalytic domain relative to the membrane plane and the interaction pattern of positively charged residues with the membrane phosphates. Specifically, in what appears to be an activation state dependent conformational exchange, the protein interacts with the DMPC phosphates through basic amino acids residing at either the catalytic domain or the linker.[12] The role of the positively charged residues in function[12] and membrane lateral segregation (D. Abankwa, personal communication) is confirmed by biochemical and biophysical experiments. Furthermore, compared to the X-ray structure, N-ras undergoes a substantial conformational change upon binding to a lipid monolayer.[22] On the other hand, it is not clear how the free ANCH would interact with the membrane. However, it has been demonstrated that ANCH fused to the Green Fluorescent Protein (GFP-ANCH) colocalizes with H-ras-GDP in ordered domains whereas HVR and H-ras-GTP colocalize in disordered domains.[13] Would these differences be manifest in protein−membrane atomic interactions and/or localizations?

Membrane Insertion and Localization of the Anchor. Figure 1B shows the progress of insertion of the minimal H-ras membrane anchor (ANCH) during a 20 ns insertion simulation (simulation *anch*, see Methods). Insertion is monitored by the number of ras-DMPC contacts, defined as the number of non-hydrogen DMPC atoms within 4 Å of non-hydrogen protein atoms. As in the earlier simulations on the HVR, H-ras-GDP and H-ras-GTP (simulations *hvr*, *fl.gdp*, and *fl.gtp*, respectively),[12] ANCH inserts and stabilizes quickly, becoming almost completely buried in the membrane after ∼5 ns (Figure 1B and C).

The normalized distribution of the position of the anchor backbone and side chains along the *z*-axis (*z*-location) is shown in Figure 2A (see also ref 12). The distribution of the backbone location in *anch* closely mimics that in *fl.gtp*. Its average location, or peak, is at $z \approx -16$ Å. For comparison, the average location of the lower leaflet phosphorus atoms is ~ -18 Å. In *fl.gdp*, the backbone inserts deeper and populates the region around the hydrophobic−hydrophilic interface (peak at ∼12 Å). The distribution in *hvr* is much wider and spans the phosphate and glycerol regions (Figure 2A). The distributions of the side chain *z*-locations (i.e., including the lipid modifications) are wide and cover $z \approx -18$ to 8, -18 to 8, -16 to 10, and -24 to 0 Å in *anch*, *hvr*, *fl.gdp*, and *fl.gtp*, respectively. For comparison, the hydrocarbon core covers $z \approx -12.5$ to 12.5 Å. Thus, the side chains populate most of the hydrocarbon core except in *fl.gtp* where they remain within the lower leaflet.

Protein−Membrane Contacts. Figure 2B displays the average number of protein non-hydrogen atoms within 4 Å of phosphate, choline, carbonyl, ester, and acyl group heavy atoms.

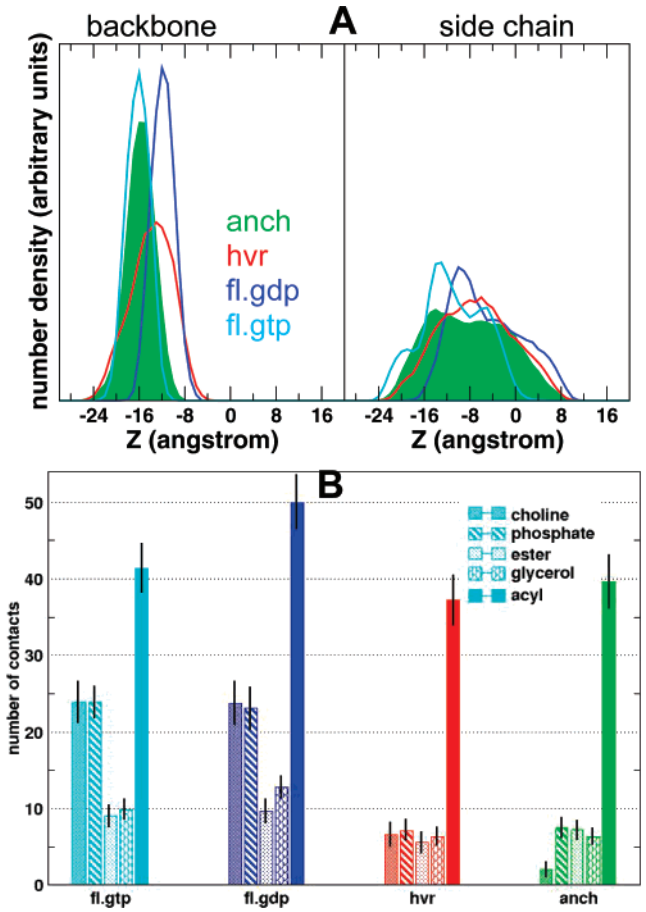

Figure 2. (A) Number density plots (along the membrane normal, *z*) of the anchor backbone (left) and side chains, including the lipid modified ones. Color code: green, simulation *anch* (anchor, residues 180−186); red, *hvr* (the hypervariable region, residues 167−186); blue, *fl.gdp* (full-length H-ras in the GDP bound form); cyan, *fl.gtp* (full-length H-ras in the GTP bound form). The bilayer is centered at $z = 0.0$. (B) Time averaged protein−DMPC contacts (see legend of Figure 1 for the definition of contact). In this and following figures, the last 15 ns of data are used.

The number of ras-choline and ras-phosphate contacts is much larger for the full-length protein (*fl.gdp* and *fl.gtp*) than for the shorter peptides (*hvr* or *anch*). This is consistent with membrane interaction of the catalytic domain in the case of *fl.gtp* and the N-terminal half (HVR1) of the linker in *fl.gdp*[12]. HVR1 is flexible in *hvr* and does not interact with the membrane. Similarly, in terms of ras-ester and ras-carbonyl contacts, the full-length proteins are approximately equal to each other and greater than the peptides. The ras-acyl contacts are within error of each other, except for the somewhat higher values in *fl.gdp*. Therefore, the average numbers of ras contacts with each DMPC chemical group do not discriminate between the two membrane binding modes of the full-length H-ras or between ANCH and HVR.

Backbone−DMPC Interactions. Backbone atoms of the anchor populate the lipid−water interface such that the amide nitrogens donate a hydrogen bond to the phosphate and/or carbonyl oxygens. The radial pair distribution functions, $g(r)$, calculated for individual anchor amide nitrogens relative to the carbonyl or phosphate oxygens are shown in Figure 3. The results indicate that backbone amides of the palmitoylated cysteines (Palm181 and Palm184) are the most potent hydrogen bond donors. Those of Met182 and Gly180 contribute to various

(20) MacKerell, A. D., et al. *J. Phys. Chem. B* **1998**, *102*, 3586−3616.
(21) Phillips, J. C.; Braun, R.; Wang, W.; Gumbart, J.; Tajkhorshid, E.; Villa, E.; Chipot, C.; Skeel, R. D.; Kale, L.; Schulten, K. *J. Comput. Chem.* **2005**, *26*, 1781−1802.
(22) Meister, A.; Nicolini, C.; Waldmann, H.; Kuhlmann, J.; Kerth, A.; Winter, R.; Blume, A. *Biophys. J.* **2006**, *91*, 1388−401.

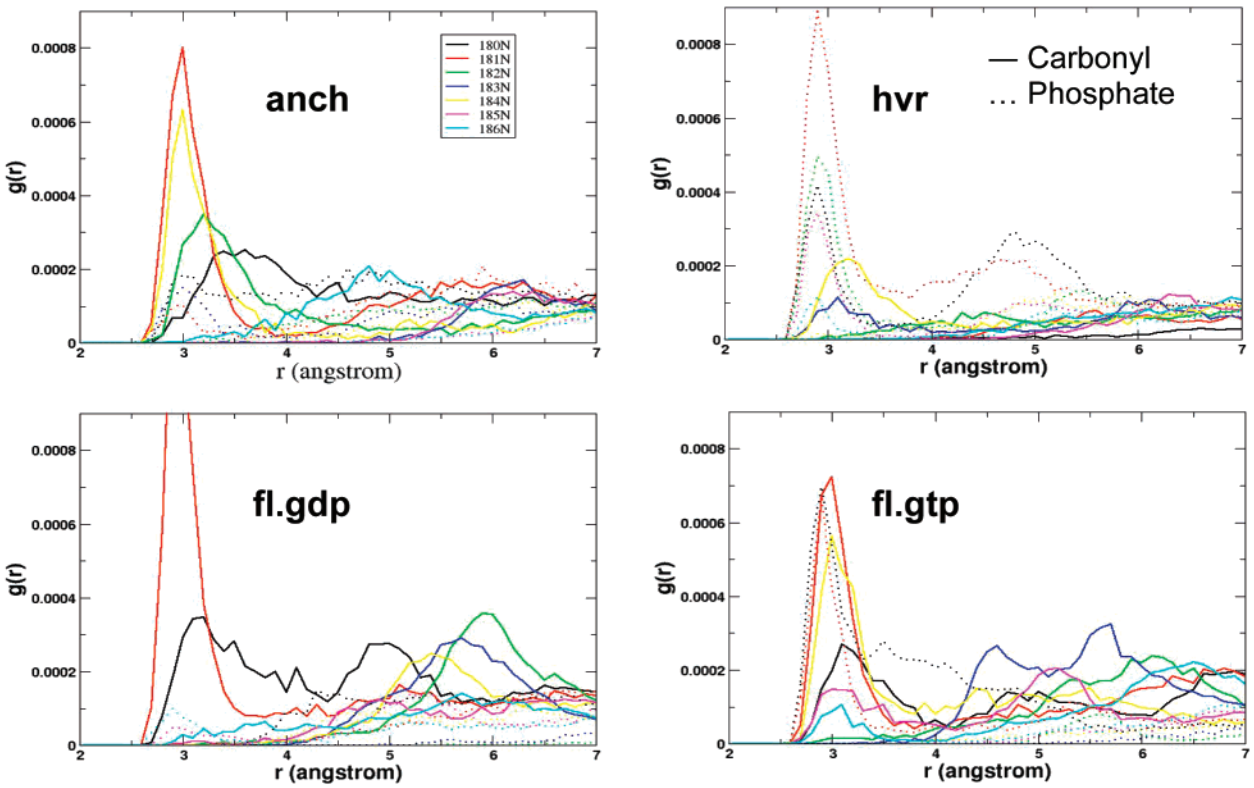

Figure 3. Radial pair distribution functions, $g(r)$, calculated for each amide nitrogen of the anchor relative to the carbonyl (solid lines) and phosphate oxygen atoms (dotted lines).

degrees, whereas the amides of Ser183 and the hexadecylated cysteine (Farn186) do not interact.

Thus, the hydrophobic residues (Palm181 and Palm184, as well as Met182 in the case of *anch* and *hvr*) have a dual contribution to membrane affinity—hydrogen bonding via an amide nitrogen and vdW interactions via a hydrophobic side chain. This raises two questions. First, why has nature chosen to incorporate polar and charged (or polar and proline in N-ras) residues in the anchor? We suggest that, due to the high desolvation cost of their burial, the polar and/or charged amino acids ensure interfacial localization and optimal orientation of the backbone by interacting with the lipid head group.[12,23] Indeed, Ser183 and Lys185 side chains hydrogen bond with the DMPC phosphates (not shown). The polarity of the backbone alone might not have been sufficient to prevent complete immersion into the hydrocarbon core. Second, why does the Farn186 amide fail to donate a hydrogen bond? The deeper insertion of Farn186 in most of the simulations (the exception being *fl.gtp*, see below) prevents effective interaction of its backbone with the polar region of the bilayer. There are two reasons for the deeper insertion. First, the C-terminal methyl group at Farn186 reduces the backbone polarity and, as a result, increases the affinity to the hydrocarbon core. In fact, absence of the methyl group resulted in a 20−40-fold (depending on the lipid composition) decrease in vesicle affinity of a monofarnesylated lipopeptide.[4] Second, the farnesyl thioether linkage renders the whole chain nonpolar. Thus, Farn186 pays less in desolvation penalty upon burial into the hydrophobic core.

There are noticeable differences among the simulations in the pattern of anchor−bilayer hydrogen bonds. For instance, Palm181 interacts with the glycerol carbonyls in all but *hvr*, where it interacts instead with the phosphate oxygen atoms. This is related to its insertion depth as, for example, the first chain carbon (C1) is farther away from the bilayer center (∼13 ± 2 Å) than in the other simulations (∼10−12 Å, Table S1). Furthermore, the amide of Palm184 is too deeply buried in *hvr* and *fl.gdp* (C1 at ∼8.0 ± 2 0.0 Å, Table S1) to be able to donate a hydrogen bond. Other differences include the interaction with the phosphate of Gly180 and Lys185 amides in simulations *hvr* and *fl.gtp* but not in *anch* and *fl.gdp*.

Overall, the backbone amides predominantly interact with the DMPC carbonyls in *anch* and *fl.gdp* simulations, with the phosphates in *hvr*, and with both in *fl.gtp*. Furthermore, the number of hydrogen bonds is higher in the latter two. These preferential interactions of the backbone loosely match the *in vivo* membrane binding behaviors mentioned earlier.

Differential Effects on Membrane Structure. Membrane structure is often perturbed by bound proteins and peptides, and these perturbations play many cellular functions.[24,25] Membrane perturbation includes local structural disturbances such as changes in thickness or lipid packing[26−28] and intrinsic thermal fluctuations[29] such as changes in peristaltic and undulatory motions.[30,31]

(23) Gorfe, A. A.; Pellarin, R.; Caflisch, A. *J. Am. Chem. Soc.* **2004**, *126*, 15277−86.
(24) Jones, M. J.; Murray, A. W. *Biochem. Biophys. Res. Commun.* **1986**, *136*, 1083−9.
(25) Halperin, A.; Mouritsen, O. G. *Eur. Biophys. J.* **2005**, *34*, 967−71.
(26) Huang, H. W. *Biochim. Biophys. Acta* **2006**, *1758*, 1292−302.
(27) Mbamala, E. C.; Ben-Shaul, A.; May, S. *Biophys. J.* **2005**, *88*, 1702−14.
(28) Jaud, S.; Tobias, D. J.; Falke, J. J.; White, S. H. *Biophys. J.* **2007**, *92*, 517−24.
(29) Lindahl, E.; Edholm, O. *Biophys. J.* **2000**, *79*, 426−33.
(30) Lee, M. T.; Chen, F. Y.; Huang, H. W. *Biochemistry* **2004**, *43*, 3590−9.
(31) Lee, M. T.; Hung, W. C.; Chen, F. Y.; Huang, H. W. *Biophys. J.* **2005**, *89*, 4006−16.

The equilibrium thermodynamic properties of the membrane in the insertion simulations were the same within error as those in a pure DMPC simulation.[12] However, the peristaltic motions of the membrane were enhanced upon binding of full-length H-ras (see Figure S1), and local perturbations have been observed.[12] Here we focus on the local perturbations. Note that experiments have shown two decades ago that normal cellular H-ras perturbs the local structure of membrane phospholipids,[32] but the atomistic detail of the mechanism has been missing.

As might be expected from "hydrophobic matching",[33] the structure of DMPC lipids in the vicinity of the longer ras lipids is perturbed (Figure 4A). Lipids near the peptide backbone are also affected. These perturbations can be characterized using the C−H bond orientational order parameter (S_{CH}), which describes the average conformations of the lipid alkyl chains as follows:

$$S_{CH} = \frac{1}{2}(\langle 3\cos^2\theta - 1\rangle)$$

here θ is the angle between the C−H bond and the membrane normal. To simplify analysis, we define two groups of lipids:[28] bound and bulk lipids. Bound lipids are defined as lipids having a non-hydrogen atom within 10 Å of any anchor non-hydrogen atom (Figure 4A). The remaining ones make up the bulk lipids. With this definition, bound lipids account, on average, for only one-fifth of all the lipids. Therefore, the overall average S_{CH} falls within the range observed for lipids in the pure bilayer, except for *fl.gtp* where it is slightly higher[12] (Figure S2). However, S_{CH} of the bound lipids is lower in *hvr* and *fl.gdp* and higher in *anch* and *fl.gtp* than that of the bulk lipids (or equivalently, than that of the pure DMPC bilayer; see Figure S2). Figure 4B plots the ras-induced change in order parameter ($\Delta S_{CH} = S_{CH}$(bound) − ΔS_{CH}(bulk)). $\Delta S_{CH} \neq 0$ implies that the membrane reduces its free energy by adjusting its (hydrophobic) thickness:[34] $\Delta S_{CH} > 0$ indicates a higher order or thickening and $\Delta S_{CH} < 0$ indicates thinning.

In its membrane-bound conformation, ANCH has its hydrophobic and polar side chains directed toward the hydrocarbon core and the aqueous phase, respectively (Figure 1A). It therefore has an amphipathic character. Membrane perturbation by amphipathic peptides varies with concentration, insertion depth, and orientation. Insertion depth is the most relevant variable here because concentration is fixed and orientation of the anchor is generally similar among the simulations. The theoretical basis for the connection between ΔS_{CH} (or the corresponding change in membrane thickness) and insertion depth has been a subject of intense investigation,[34,35] especially in connection with antimicrobial peptides.[31,36,37] For example, it has been shown that a rigid amphipathic peptide horizontally embedded in a membrane of 26 Å hydrophobic thickness results in $\Delta S_{CH} > 0$ or $\Delta S_{CH} < 0$ depending on whether it is partially or fully inserted in the hydrocarbon core, respectively.[34] The current simulation results are qualitatively consistent with this pattern. In *anch* and *fl.gtp*, the backbone resides at the head group−water interface (average distance from bilayer center, $z \approx 16$ Å, Figure 2A) and $\Delta S_{CH} > 0$. The corresponding changes in membrane thickness (ΔD_{PP}, the difference between bound and bulk lipids in terms of average separation of phosphorus atoms at the two leaflets) are +1.7 and +2.7 Å, respectively. In simulations *hvr* and *fl.gdp*, the backbone is at the hydrophobic−hydrophilic interface ($z \approx 12 - 13$ Å) and $\Delta S_{CH} < 0$, with corresponding ΔD_{PP} values of −3.6 and −1.4 Å. A similar effect by the peptide fragment from the intracellular domain of the HIV-1 gp41 protein has been observed experimentally.[38] These local perturbations may provide a hint into the early stages of ras-assisted membrane nanoclustering.[18,19]

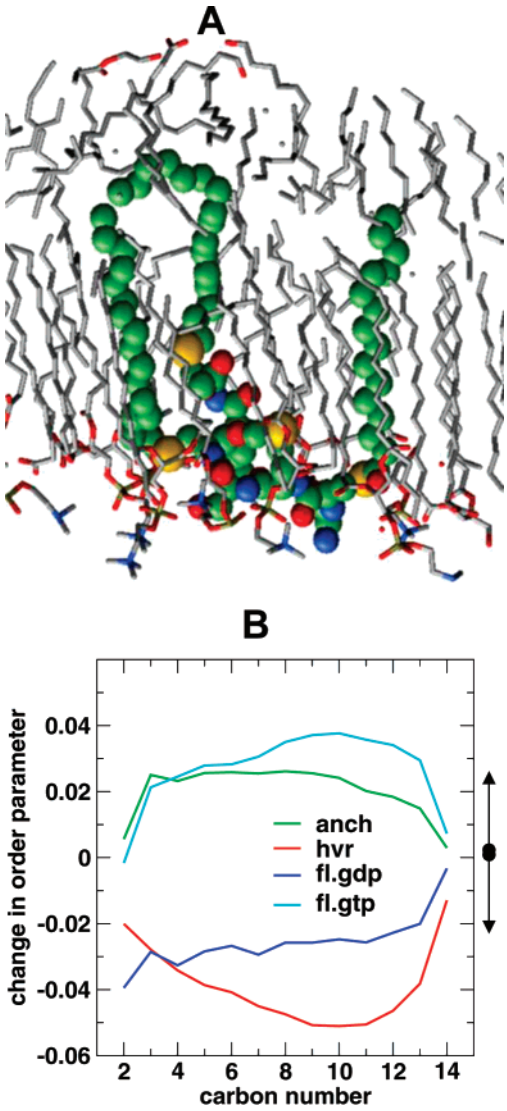

Figure 4. (A) Membrane structural perturbation upon insertion of ANCH. Non-hydrogen atoms of DMPC lipids within 10 Å of any ANCH non-hydrogen atom are shown in a stick model with oxygen in red, nitrogen in blue, and carbon in gray. The last snapshot from simulation *anch* is used in this figure. Notice the deformation of the lipid tails at the peptide-bound lower leaflet as well as the upper leaflet. The 10 Å cutoff used is arbitrary, but tests at 5 and 15 Å showed that the former did not include all affected lipids while the latter is dominated by bulk-like lipids. (B) Change in the orientational order parameter (S_{CH}, see Figure S2) calculated as the difference in S_{CH} between the bound and bulk lipids (S_{CH}(bound) − S_{CH}(bulk)). Bound lipids are defined as lipids having a non-hydrogen atom within 10 Å of any ANCH non-hydrogen atom. The rest are defined as bulk lipids. The arrows at the right *y*-axis indicate an increase (up) and decrease (down) of membrane thickness accompanying the changes in the chain order.

(32) Montgomery, G. W.; Jagger, B. A.; Bailey, P. D. *Biochemistry* **1988**, *27*, 4391−5.
(33) Huang, H. W. *Novartis Found. Symp.* **1999**, *225*, 188−200; discussion 200−6.
(34) Zemel, A.; Ben-Shaul, A.; May, S. *Biophys. J.* **2004**, *86*, 3607−19.
(35) Zemel, A.; Ben-Shaul, A.; May, S. *Eur. Biophys. J.* **2005**, *34*, 230−42.
(36) Heller, W. T.; Waring, A. J.; Lehrer, R. I.; Harroun, T. A.; Weiss, T. M.; Yang, L.; Huang, H. W. *Biochemistry* **2000**, *39*, 139−45.
(37) Chen, F. Y.; Lee, M. T.; Huang, H. W. *Biophys. J.* **2003**, *84*, 3751−8.

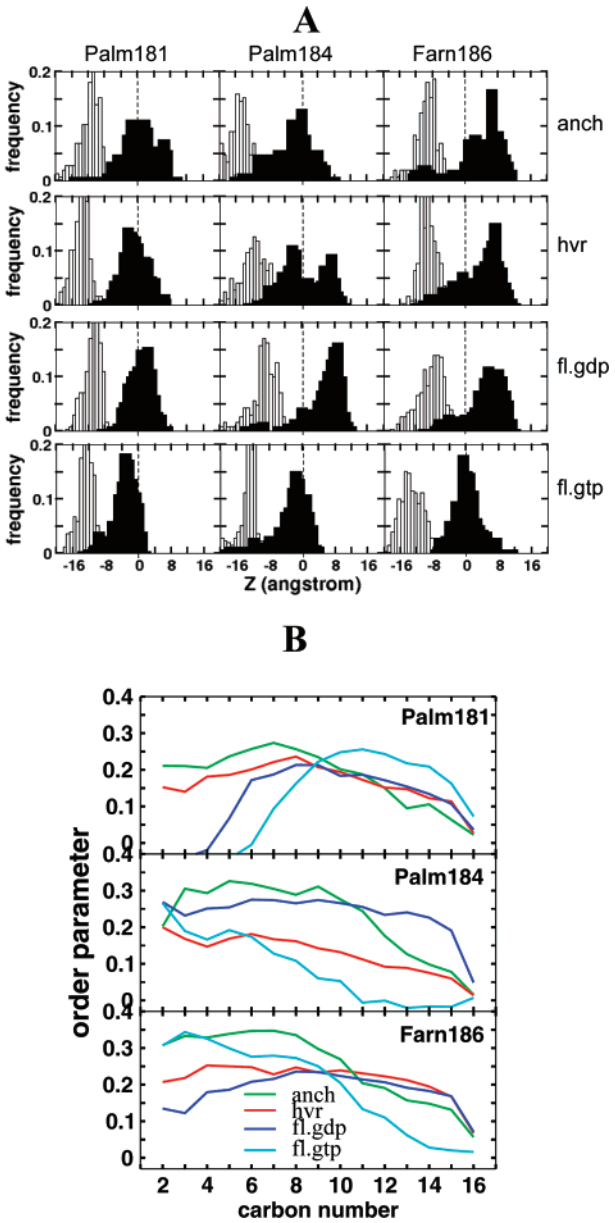

Figure 5. (A) Histograms of *z*-locations of the first (C1, open bars) and last (C16, solid bars) tail carbon atoms of ras lipids. (B) Order parameters of the ras lipid chains.

Interface-bound antimicrobial peptides cause membrane thinning because they displace lipid headgroups and thereby create a vacant space underneath them.[26,31,39−42] To fill up this space, lipids at the peptide-containing monolayer splay and tilt while lipids at the opposite monolayer stretch. In the case of the H-ras anchor, a combination of its backbone localization and the chain length of its lipid modifications modulate the membrane thickness. Thus, in *fl.gtp*, the hexadecyl group is extended (average chain length ∼14 Å) with its backbone near the phosphate group (average C1 position 15.6 ± 2 Å; Figures 5 and S2 and Table 1). Palm181 and Palm184 are flexible (chain length ∼9.3 and 10.7 Å) with their C1 colocalizing with those of the DMPC. On average, however, the chain length of the ras lipids roughly matches that of the lower leaflet lipids. Hence, the increase in membrane thickness is mainly caused by the interface localized backbone. In *fl.gdp*, a section of each ras lipid tail crosses the bilayer center and interacts with lipids of the opposite leaflet, which become flexible to achieve hydrophobic matching. Thus membrane thinning in *fl.gdp* can be mainly attributed to the ras lipid tails. The process is more complicated in *anch* and *hvr* although on average the backbone and the lipid tails play a predominant role, respectively (Figure 5 and Table S1). Note that in contrast to the full-length ras where the effect on the lower leaflet is damped, both leaflets are affected in *anch* and *hvr*.

The variations in the palmitoyl and hexadecyl chain lengths discussed above are reflected in their order parameters. If we compare the mean (i.e., averaged over all the carbon atoms) order parameter ($\bar{S}_{CH}$) of the DMPC lipids and the ras lipids as $m \equiv (\bar{S}_{CH})^{ras} - (\bar{S}_{CH})^{DMPC}$, we find that the latter are slightly more ordered in ANCH ($m = +0.02$), slightly less ordered in HVR and H-ras-GDP ($m = -0.03$), and substantially less ordered in H-ras-GTP ($m = -0.07$). The order in ANCH is in contrast to the flexibility in the dually lipidated N-ras heptapeptide ($m = -0.06$).[23,43] Furthermore, there is a dramatic difference of mobility between the two palmitoyls and between the palmitoyl and the hexadecyl chains (Figure 5B). Note also that Palm184 is significantly more flexible in HVR and H-ras-GTP than in ANCH and H-ras-GDP. The first six carbon atoms of Palm181 are completely disordered in the full-length H-ras.

Concluding Remarks

A number of biophysical and biochemical experiments demonstrated that ANCH stably binds to the plasma membrane[13,15] and its membrane lateral segregation is modulated by the catalytic domain and the linker.[13,15,16,18,44−46] Our simulations show that (i) ANCH quickly inserts and stabilizes in the bilayer (Figure 1B and C) and (ii) the insertion depth of its lipids and the localization of its backbone is modulated by the linker and the catalytic domain (Figures 2−5). The large difference in size and time scales between the simulations and the experiments limits direct comparison. Nonetheless, some useful lessons can be drawn from a qualitative comparison.

First, experimentally the membrane lateral segregation GFP-fused ANCH and H-ras-GDP is cholesterol-sensitive while that of HVR and H-ras-GTP is not cholesterol-sensitive.[13] In the simulations, Palm184 is more ordered in ANCH and H-ras-GDP than in HVR and H-ras-GTP (Figure 5, Table S1). Palm184 has been implicated as the primary source of differential membrane segregation.[15] Furthermore, the backbone of HVR and H-ras-GTP makes hydrogen bonds predominantly with phosphate oxygen atoms while the backbone of ANCH and H-ras-GDP interact with the glycerol oxygen atoms. However, ANCH and H-ras-GTP behave similarly to each other— and oppositely from HVR and H-ras-GDP—in back-

(38) Koenig, B. W.; Ferretti, J. A.; Gawrisch, K. *Biochemistry* **1999**, *38*, 6327−34.
(39) Jang, H.; Ma, B.; Woolf, T. B.; Nussinov, R. *Biophys. J.* **2006**, *91*, 2848−59.
(40) Sato, H.; Feix, J. B. *Biochim. Biophys. Acta* **2006**, *1758*, 1245−56.
(41) Mecke, A.; Lee, D. K.; Ramamoorthy, A.; Orr, B. G.; Banaszak, Holl, M. M. *Biophys. J.* **2005**, *89*, 4043−50.
(42) Bainbridge, J.; Jones, N.; Walker, B. *Clin. Exp. Immunol.* **2004**, *137*, 298−304.
(43) Huster, D.; Vogel, A.; Katzka, C.; Scheidt, H. A.; Binder, H.; Dante, S.; Gutberlet, T.; Zschornig, O.; Waldmann, H.; Arnold, K. *J. Am. Chem. Soc.* **2003**, *125*, 4070−9.
(44) Hancock, J. F.; Parton, R. G. *Biochem. J.* **2005**, *389*, 1−11.
(45) Parton, R. G.; Hancock, J. F. *Trends Cell. Biol.* **2004**, *14*, 141−7.
(46) Prior, I. A.; Harding, A.; Yan, J.; Sluimer, J.; Parton, R. G.; Hancock, J. F. *Nat. Cell Biol.* **2001**, *3*, 368−75.

bone localization and membrane perturbation (Figures 2−5, S1−S2). Among a number of potential reasons for this apparent discrepancy, one may be that membrane binding by the short peptides HVR and ANCH is somewhat different in the GFP-fused form. Another could be the choice of lipids or limited sampling in the simulations.

Second, binding of ras at the inner monolayer consistently perturbs the outer monolayer. This implies that ras affects and may be affected by the outer leaflet of the plasma membrane which has a lipid composition that allows for spontaneous formation of lateral heterogeneity.

Third, from the interfacial localization of the backbone, especially Palm184, in ANCH and H-ras-GTP relative to the deeper insertion in HVR and H-ras-GDP (Figures 2&5 and Table S1), one may ask whether such a mechanism controls accessibility to palmitoylthioesterases.[10]

Finally, regarding differences in the cholesterol sensitivity of GDP and GTP loaded ras, three alternative—but partially interdependent—explanations may be forwarded. The first of which takes into account the fact that membrane thinning by antimicrobial peptides leads to destruction of bacterial membranes.[47] Membrane thinning by cellular H-ras with a potentially similar consequence may force H-ras-GDP to segregate to cholesterol-rich ordered domains in order to relieve the membrane stress. A similar idea was forwarded before based on the insertion depth and ordering of the ras lipids.[12,48] The second alternative is to consider that the backbone of H-ras-GDP and the OH of cholesterol interact with the carbonyls of membrane lipids in what is called the "umbrella model" of cholesterol-phospholipid interaction, where the OH of cholesterol is covered over by the headgroups.[49] Cholesterol and H-ras-GDP may therefore cluster together by complementing each other in reducing the cost of membrane deformation accompanying their preferred mode of binding. On the other hand, the membrane thickening observed in H-ras-GTP may be viewed as activated ras having a condensing role similar to that of cholesterol. Thus, both H-ras-GTP and H-ras-GDP sit at thicker locales by directly thickening their vicinity or by migrating to and/or colocalizing with cholesterol-rich regions, respectively. This model predicts that in the cell both the activated and cellular H-ras help form and cluster within membrane nanodomains by thickening the membrane in their vicinity and subsequently clustering at high curvature regions. This is consistent with recent experiments that indicated accumulation of cholesterol in high curvature regions.[50] The third alternative stems from the negative spontaneous curvature of cholesterol[51] and its interaction with regions of negative curvature. Thus, the local membrane deformation, i.e., the negative curvature of the upper monolayer induced by H-ras-GDP, may explain the cholesterol-sensitive membrane lateral segregation of GDP loaded H-ras. In order to determine which of these mechanisms is applicable, it would be necessary to investigate the role of cholesterol, lipid composition, etc., as well as the water-to-membrane transfer free energy of ras. Some of these issues are currently under study in our lab. As an example, our recently calculated potential of mean force for the insertion of ANCH into a DMPC bilayer indicates a steeply downhill profile and a free energy change of ∼30 kcal/mol.[52] The decomposition of the free energy into enthalpic and entropic effects, the contribution of individual lipid modifications, and the role of water are some of the interesting questions awaiting further computational and experimental scrutiny.

Acknowledgment. A.A.G. acknowledges financial support from the Commission for the Promotion of Young Academics of the University of Zurich. We thank Dr. M. Hanzal-Bayer for very constructive suggestions on the manuscript, Prof. J. F. Hancock, Drs. D. Abankwa, and I. Ivanov for discussions, the San Diego Super Computer Center and the Center for Theoretical Biological Physics for computational resources. Additional support has been provided by the National Science Foundation, National Institutes of Health, Howard Hughes Medical Institute, National Biomedical Computation Resource, and Accelrys Inc.

Supporting Information Available: Table S1 containing the mean (and standard deviation) of the C1 and C16 atoms locations, along the *z*-axis, of the ras palmitoyl and hexadecyl chains; Figure S1 showing density plots for 10 Å running averages of the instantaneous membrane thickness along the *x* and *y* directions (a), and the time evolution of the change in membrane thickness along the *x*-axis (b); Figure S2 showing orientational order parameters computed for bound and bulk lipids per leaflet; complete ref 20. This material is available free of charge via the Internet at http://pubs.acs.org.

JA073949V

(47) Zasloff, M. *Nature* **2002**, *415*, 389−95.
(48) Abankwa, D.; Gorfe, A. A.; Hancock, J. F. *Semin. Cell Dev. Biol.* **2007**, *18*, in press.
(49) Ali, M. R.; Cheng, K. H.; Huang, J. *Proc. Natl. Acad. Sci. U.S.A.* **2007**, *104*, 5372−7.
(50) Wang, W.; Yang, L.; Huang, H. W. *Biophys. J.* **2007**, *92*, 2819−30.
(51) Chen, Z.; Rand, R. P. *Biophys. J.* 1**997**, *73*, 267−76.
(52) Gorfe, A. A.; Babakhani, A.; McCammon, J. A. *Angew. Chem., Int. Ed.* **2007**, in press.